



# Trophoblast Side-Population Markers are Dysregulated in Preeclampsia and Fetal Growth Restriction

Georgia P. Wong<sup>1,2</sup> · Sunhild Hartmann<sup>1,2,3,4,5,6</sup> · David G. Simmons<sup>7</sup> · Sarah Ellis<sup>8,9</sup> · Olivia Nonn<sup>3,4,5,6,10</sup> · Ping Cannon<sup>1,2</sup> · Tuong-Vi Nguyen<sup>1,2</sup> · Anna Nguyen<sup>1,2</sup> · Lucy A. Bartho<sup>1,2</sup> · Stephen Tong<sup>1,2</sup> · Natalie J. Hannan<sup>1,2</sup> · Tu'uhevaha J. Kaitu'u-Lino<sup>1,2</sup>

Accepted: 10 July 2024  
© The Author(s) 2024

## Abstract

Dysregulated progenitor cell populations may contribute to poor placental development and placental insufficiency pathogenesis. Side-population cells possess progenitor properties. Recent human trophoblast side-population isolation identified enrichment of 8 specific genes (*CXCL8*, *ELL2*, *GATA6*, *HK2*, *HLA-DPB1*, *INTS6*, *SERPINE3* and *UPP1*) (Gamage et al. 2020, *Stem Cell Rev Rep*). We characterised these trophoblast side-population markers in human placenta and in placental insufficiency disorders: preeclampsia and fetal growth restriction (FGR). Trophoblast side-population markers localised to mononuclear trophoblasts lining the placental villous basement membrane in preterm control, preeclamptic and FGR placental sections ( $n = 3$ , panel of 3 markers/serial section). Analysis of single-cell transcriptomics of an organoid human trophoblast stem cell (hTSC) to extravillous trophoblast (EVT) differentiation model (Shannon et al. 2022, *Development*) identified that all side-population genes were enriched in mononuclear trophoblast and trophoblasts committed to differentiation under hTSC culture conditions. *In vitro* validation via 96 h time course hTSC differentiation to EVTs or syncytiotrophoblasts ( $n = 5$ ) demonstrated *ELL2* and *HK2* increased with differentiation ( $p < 0.0024$ ,  $p < 0.0039$  respectively). *CXCL8* and *HLA-DPB1* were downregulated ( $p < 0.030$ ,  $p < 0.011$  respectively). *GATA6* and *INTS6* increased with EVT differentiation only, and *UPP1* reduced with syncytialisation. *SERPINE3* was undetectable. Trophoblast side-population marker mRNA was measured in human placentas (< 34-weeks' gestation;  $n = 78$  preeclampsia,  $n = 30$  FGR, and  $n = 18$  gestation-matched controls). *ELL2*, *HK2* and *CXCL8* were elevated in preeclamptic ( $p = 0.0006$ ,  $p < 0.0001$ ,  $p = 0.0335$  respectively) and FGR placentas ( $p = 0.0065$ ,  $p < 0.0001$ ,  $p = 0.0001$  respectively) versus controls. Placental *GATA6* was reduced in pregnancies with preeclampsia and FGR ( $p = 0.0014$ ,  $p = 0.0146$  respectively). Placental *INTS6* was reduced with FGR only ( $p < 0.0001$ ). This study identified the localisation of a unique trophoblast subset enriched for side-population markers. Aberrant expression of some side-population markers may indicate disruptions to unique trophoblast subtypes in placental insufficiency.

**Keywords** Trophoblast · Placenta · Preeclampsia · Fetal growth restriction · Pregnancy

✉ Georgia P. Wong  
gpwong@student.unimelb.edu.au

<sup>1</sup> The Department of Obstetrics, Gynaecology and Newborn Health, Mercy Hospital for Women, University of Melbourne, 163 Studley Road, Heidelberg, Victoria 3084, Australia

<sup>2</sup> Mercy Perinatal, Mercy Hospital for Women, Heidelberg, Victoria, Australia

<sup>3</sup> Charité – Universitätsmedizin Berlin, corporate member of Freie Universität Berlin and Humboldt-Universität, Berlin, Germany

<sup>4</sup> Experimental and Clinical Research Center, a cooperation between the Max-Delbrück-Center for Molecular Medicine in the Helmholtz Association and the Charité - Universitätsmedizin Berlin, Berlin, Germany

<sup>5</sup> Max-Delbrück-Center for Molecular Medicine in the Helmholtz Association (MDC), Berlin, Germany

<sup>6</sup> DZHK (German Center for Cardiovascular Research), partner site Berlin, Berlin, Germany

<sup>7</sup> School of Biomedical Sciences, University of Queensland, Brisbane, Australia

<sup>8</sup> Olivia Newton-John Cancer Research Institute, Heidelberg, VIC 3084, Australia

<sup>9</sup> School of Cancer Medicine, La Trobe University, Melbourne, VIC 3086, Australia

<sup>10</sup> Division of Cell Biology, Histology and Embryology, Gottfried Schatz Research Center, Medical University of Graz, Graz, Austria

## Introduction

The placenta represents the life-support system for a fetus throughout pregnancy. Aberrant placentation may trigger downstream dysfunction, conferring poor nutrient perfusion and vulnerability to the development of placental insufficiency. Preeclampsia and fetal growth restriction (FGR), two prevalent placental insufficiency disorders, can lead towards poor obstetric outcome. Each disease affects between 3–8% of pregnancies worldwide, with an inequitable distribution amongst low-resource settings [1]. In preeclampsia, placental malperfusion incites endothelial dysfunction in the maternal systemic vasculature, manifesting clinically as maternal hypertension and end-organ dysfunction [2]. In FGR, restricted placental function results in the fetus failing to reach its genetically pre-determined growth potential *in utero* [3]. FGR is the largest standalone risk factor for stillbirth, with perinatal survival predisposing to lifelong elevated incidences of morbidity and mortality [3]. These two disorders can occur in isolation or in unison, suggesting some elements of molecular mechanisms may be shared. Understanding placental insufficiency pathogenesis is crucial to developing preventative and therapeutic measures that will alleviate the existing and extensive burden of disease.

The placenta facilitates the control of nutrient and waste exchange and is a proxy for developing fetal organs. Therefore, establishment and maintenance of its trophoblast (placental epithelia) sub-populations are critical to a healthy pregnancy. To date, much research effort has focused on understanding the terminal trophoblast phenotypes and their functions. However, more recent attention has been focused on the existence and identification of a distinct pool of placental progenitor cells. Should these progenitor pools become dysregulated, perturbations in differentiation trajectories to mature trophoblast phenotypes may ensue, contributing to placental insufficiency. Identifying and investigating molecular markers that provide indication of these niche cell populations may therefore serve to uncover their roles in placental development and physiology as well as in pathological conditions. These may aid in identifying opportunities to improve detection and intervention for pregnancy complications.

Once classical epithelial progenitor cells commit to a cell fate, they transform into intermediate progenitor cells that undergo rapid proliferation in a process termed ‘transit amplification’ [4, 5]. Historical concepts referred to mononuclear cytotrophoblasts as a bipotential progenitor trophoblast population, however; more recent data suggests that there are likely multiple subpopulations of cytotrophoblasts, with each representing commitment to a more terminally differentiated trophoblast lineage [6, 7].

These differentiated lineages include invasive extravillous trophoblasts (EVTs) and multinucleated syncytiotrophoblasts. Collectively, trophoblasts act to anchor the placenta to the maternal decidua during pregnancy, induce remodelling and by extension enhance capacitance of the maternal blood flow. They also form a specialised transporting barrier, allowing effective maternal–fetal exchange.

Side-population cells are a cell population, that demonstrate progenitor properties of self-renewal and potency, and are enriched for progenitor and stem cell surface markers [8]. They are isolated by excluding the DNA-binding fluorescent Hoechst 33342 dye via expression of ATP-binding cassette cell membrane transporter proteins [9, 10]. Flow cytometry sorts the ‘Hoechst-low’ population, that appears to the ‘side’ of other cell populations, explaining their distinction as ‘side-population’ cells. Recently, the Hoechst 33342 technique yielded ‘side-population trophoblasts’ from the placenta [11]. Side-population trophoblasts persist across all trimesters of pregnancy, with reduced abundance in FGR-affected placentas [12]. This trophoblast population was postulated to include the resident placental progenitor cell population that may be dysregulated in FGR pathogenesis [12]. Isolated side-population trophoblasts are transcriptionally distinct, with increased expression of 8 genes: C-X-C motif chemokine ligand 8 (*CXCL8*)/interleukin-8 (*IL8*), elongation factor for RNA polymerase II 2 (*ELL2*), GATA-binding factor 6 (*GATA6*), hexokinase 2 (*HK2*), HLA class II histocompatibility antigen DP  $\beta$  chain 1 (*HLA-DPB1*), integrator complex subunit 6 (*INTS6*), serpin family E member 3 (*SERPINE3*), uridine phosphorylase 1 (*UPP1*). However, identification of where these side-population cells reside in placenta remains unknown.

This study aimed to localise the trophoblast side-population cells through expression of their distinct markers in human placenta via multiplexed immunofluorescence (mIF), single-cell transcriptomics, and *in vitro* differentiation studies. Once cell types were discerned, dysregulation of the proposed side-population trophoblast marker panel in human placental lysates were assessed. This sought to shed light on disruption to the establishment and maintenance of placental cell populations that may contribute to placental insufficiency and adverse perinatal outcomes, namely preeclampsia and fetal growth restriction.

## Methods

### Opal™-tyramide Signal Amplification (TSA) Multiplexed Immunofluorescence (mIF) and Image Analysis

The grouping and order of antibodies in each panel were determined with the following considerations: 1) Each

antibody required pairing with a fluorophore. Less abundant markers were matched to brighter fluorophores (Opal™ 520 – CXCL8, HLA-DPB1), intermediate abundance (Opal™ 570 – UPP1, INTS6) and more abundant markers were paired with dimmer fluorophores (Opal™ 690 – SERPINE3, HK2). 2) The effects of the number of rounds of heat-induced epitope retrieval (HIER) can degrade or enhance epitope exposure and subsequent staining. This was determined by each antibody stained on serial sections that were subject to either 1 or 3 rounds of HIER. Antibodies that were degraded with multiple HIER treatments resulted in later application and vice versa. 3) To mitigate incomplete stripping between HIER treatments, antibodies localising to the same subcellular compartments (for example, cytoplasm or nucleus), were not applied sequentially [13]. The resulting fluorophore pairings and staining order were as follows: Panel 1 labelled on one serial section) SERPINE3-Opal™ 690, HLA-DPB1-Opal™ 520, and UPP1-Opal™ 570. Panel 2 labelled on a second serial section) HK2-Opal™ 690, CXCL8-Opal™ 520, and INTS6-Opal™ 570. Once optimised, Opal™ multiplexed immunofluorescence (mIF) staining [14] was conducted on formalin-fixed paraffine-embedded (FFPE) sections. Single marker controls were additionally run to ensure consistency between individual and mIF stains. Paraffin embedded placental samples ( $n=3$  biological replicates of placentas obtained from pregnancies that delivered with preeclampsia, FGR or preterm gestation-matched controls) were serial sectioned at 4  $\mu\text{m}$  and collected on SuperFrost™ Plus adhesion microscope slides (ThermoFisher Scientific™). Sections were dried at room temperature overnight. Placental sections were deparaffinised and rehydrated as follows: xylene three times, 100% ethanol twice, 70% ethanol for 3 min each; distilled water 1 min. Side-population markers were localised with the Opal 6-Plex Detection Kit (Akoya Biosciences®, Massachusetts, US) as per manufacturer's instructions. BLOXALL® Endogenous Blocking Solution and ImmPRESS® HRP Universal Antibody (Vector Laboratories, California, US) were used as an endogenous peroxidase blocking and secondary antibody respectively. The following primary antibodies were utilised each with application at 4 °C overnight: anti-CXCL8 (anti-IL8, Abcam, Cambridge, UK, Cat#Ab106350), anti-HK2 (ThermoFisher Scientific™, Cat#PA5-29326), anti-HLA-DPB1 (Abcam, Cat#Ab157210), anti-INTS6 (Sigma-Aldrich, Missouri, US, Cat#HPA001846), anti-SERPINE3 (Novus Biologicals, Minnesota, US, Cat#NBP2-34209) and anti-UPP1 (Novus Biologicals, Cat#NBP2-30852). Antibodies for ELL2 (Novus Biologicals, Cat#NBP2-55603) and GATA6 (Bio-Techne, Minnesota, US, Cat#AF1700) were unable to be optimised due to limited antibody specificity. Immunofluorescence tyramide signal amplification (TSA) dyes Opal™ 520, Opal™ 570 and Opal™ 690 and counterstaining with Spectral DAPI were applied. Slides were

imaged using the Vectra® Polaris™ 3.0 Automated Quantitative Pathology Imaging System, 200 slide (Perkin Elmer, Massachusetts, US). Whole slide analysis was performed for each section at 10 $\times$  magnification using the HALO® Image Analysis Platform's Highplex FL module v4.1.3 (Indica Labs, Albuquerque, US).

### Single-cell RNA Sequencing (scRNA-seq) of an hTSC-derived Organoid Model for Trophoblast Differentiation

To analyse scRNA-seq data, the code previously published (<https://github.com/MatthewJShannon>) was applied on the dataset (GEO accession number GSE174481) for the pre-processing steps and adjusted for subsequent analysis [15].

Using the Seurat R package (version 5.0.1) [16, 17], 8228 cells were used for pre-processing of the data including doublet removal with DoubletFinder package version 2.0.4 [18]. The remaining 6354 cells were used for downstream analysis. Downstream analysis was performed as previously described [15] including integration of all 6 samples ( $n=3$  biological replicates for each condition), normalisation and single-cell transcriptomics transformation with subsequent clustering using the FindCluster function at a resolution of 1. Dimensionality reduction was performed using the runUMAP function with 33 principal components. Characteristic marker genes for each cell type were used to annotate clusters. Each cluster was annotated with 1 of the following 6 cell identities: mononuclear trophoblast (MNT), characterised by expression of paternally expressed 10 (*PEG10*) and tumour protein 63 (*TP63*); proliferative mononuclear trophoblast (MNTprol) by marker of proliferation Ki-67 (*MKI67*) [19–21], pre-fusion mononuclear trophoblast (MNTpf) by endogenous retrovirus (ERV) group W member 1, ERV group FRG member 1, ERV group V member 1 (*ERVW-1*, *ERVFRD-1*, *ERVV-1*), progenitor EVT (pEVT) by *MKI67*, centromere protein K (*CENPK*), integrin subunit  $\alpha$  2 (*ITGA2*), human leukocyte antigen G (*HLA-G*); invasive EVTs (iEVT) by *ITGA2*, *HLA-G*, matrix metalloproteinase 2 (*MMP2*), v-erb-b2 avian erythroblastic leukemia viral oncogene homolog 2 (*ERBB2*), placenta-specific 8 (*PLAC8*); and syncytiotrophoblasts (STB) by major facilitator superfamily domain-containing protein 2 (*MFS2A*) and cytochrome P450 aromatase (*CYP19A*) [20, 22–27]. General trophoblast markers: epidermal growth factor receptor, keratin 7, transcription factor AP-2  $\gamma$ , GATA binding protein 3 (*EGFR*, *KRT7*, *TFFA2C*, *GATA3* respectively) were also applied [28, 29]. After cluster annotation, a data subset was created based on EVT-differentiated and undifferentiated samples. Dot plot and feature plots based on the single gene expression and module scores using the AddModuleScore function were generated for the genes *CXCL8* (*IL8*), *ELL2*, *GATA6*, *HK2*, *HLA-DPB1*, *INTS6*, *SERPINE3*, *UPP1* to visualize

their respective expression. The full code is available upon request.

### Culture of Human Trophoblast Stem Cells

A human trophoblast stem cell (hTSC, CT30, female) line was imported from the RIKEN BioResource Research Center via the National BioResource Project of MEXT/AMED, Japan (RCB Cat#RCB4938, RRID: CVCL\_A7BB) [30]. 24 h after plating, hTSCs were cultured in cell culture media that induced differentiation to either extravillous trophoblasts (EVTs) or syncytiotrophoblasts for 96 h. Cell lysates were collected for RNA extraction and subsequent gene analysis at 0, 48 and 96 h post-introduction to differentiation media. Cell culture experiments were run in technical duplicates and repeated  $n=5$  times (as biological replicates).

### Placental Lysates: Early Onset Preeclampsia & Fetal Growth Restriction

Placental samples were sourced from the Mercy Hospital for Women Tissue Bank (Heidelberg, Victoria, Australia). Samples were donated following informed, written consent. This study was approved by the Mercy Health Human Research Ethics Committee (R11/34).

Placental tissue was obtained from patients who delivered with early-onset preeclampsia (< 34 weeks' gestation,  $n=61$  biological replicates), FGR ( $n=12$ ) or both ( $n=18$ ), compared to placentas collected from gestation-matched control pregnancies ( $n=18$ ). Control placentas originated from deliveries with normal birth weight centile (> 10th centile for gestational age) that were normotensive and unaffected by chorioamnionitis, as confirmed by placental histopathology. Diagnoses of preeclampsia were made according to the American College of Obstetricians and Gynecologists (ACOG) guidelines (2020) [31]. FGR was defined as < 10th birthweight centile on local birthweight charts [32]. All placentas were obtained as outlined prior [33]. For participant characteristics, refer to Supplementary Table II (Placental RNA < 34 weeks' gestation).

### RNA Isolation

The GenElute™ mammalian total RNA miniprep kit (Sigma-Aldrich) was used to isolate RNA from placental samples and hTSCs as per manufacturer's instructions. mRNA concentration quantification was conducted with the Nanodrop ND 1000 spectrophotometer (NanoDrop Technologies Inc), and equivalent amounts converted to cDNA as described below.

### Quantitative Reverse Transcriptase Polymerase Chain Reaction (qRT-PCR)

RNA was reverse transcribed into cDNA with the High-Capacity cDNA Reverse Transcriptase Kit (Applied Biosystems, Massachusetts, US) as per the manufacturer's instructions. For gene expression, the primers used to target each gene were as follows: *CXCL8* (Assay ID: Hs00174103\_m1), *ELL2* (Assay ID: Hs00831747\_s1), *GATA6* (Assay ID: Hs00231122), *HK2* (Assay ID: Hs00606086\_m1), *HLA-DPB1* (Assay ID: Hs03045105\_m1), *INTS6* (Assay ID: Gs00247179\_m1), *SERPINE3* (Assay ID: Hs01391001\_m1), *UPP1* (Assay ID: Hs01066247\_m1), TEA domain transcription factor 4 (*TEAD4*, Assay ID: Hs01125032\_m1), human leukocyte antigen G (*HLA-G*, Assay ID: Hs03045108\_m1), and syndecan-1 (*SDC1*, Assay ID: Hs00896423\_m1). Gene expression was quantified through the CFX384 Touch Real Time PCR Detection System (Bio-Rad, California, US) with 10  $\mu$ L reactions consisting of fluorescein (FAM)-labelled TaqMan Fast Advanced Master Mix (ThermoFisher Scientific™, Massachusetts, US) and each specific primer (Life Technologies, California, US). Quantitative reverse transcriptase polymerase chain reactions (qRT-PCRs) were performed under the conditions as follows: 95° for 20 s, with 40 subsequent amplification cycles to denature for 3 s at 95 °C, with annealing for 30 s at 60 °C. No product was detected in non-template controls. Gene expression was calculated as the geometric mean of cytochrome C1 (*CYCI*, Assay ID: Hs00357717\_m1) and DNA topoisomerase I (*TOPI*, Assay ID: Hs00243257\_m1) for placental samples, or for *in vitro* studies, glyceraldehyde 3-phosphate dehydrogenase (*GAPDH*) was used for hTSC differentiation to syncytiotrophoblasts, while *CYCI* was utilised for hTSC differentiation to EVT. Samples were run as technical duplicates, with the average threshold (Ct) value used. Gene expression was normalised to the mean Ct of each control group, with analysis conducted via the  $2^{-\Delta\Delta Ct}$  method.

### Statistical Analysis

All *in vitro* experiments were performed with technical duplicates and repeated five times (as biological replicates) unless stated otherwise. Normality and lognormality tests (Anderson-Darling test, D'Agostino and Pearson test, Shapiro-Wilk test, and Kolmogorov-Smirnov test) were conducted to select statically appropriate tests. Data with two unpaired groups were analysed with either an unpaired *t*-test (parametric) or Mann-Whitney test (non-parametric). Analysis of data with more than three groups were analysed with one-way ANOVA (parametric) or Kruskal Wallis tests (non-parametric) with post-hoc analyses to identify differences. Significance value of  $p < 0.05$  was used. All statistical



analyses were performed on Graph Prism 10.1.0 (GraphPad Software Inc, California, US).

## Results

### Opal™-tyramide Signal Amplification (TSA) Multiplexed Immunofluorescence (mIF) in Placental Sections from Human Preterm Controls, and Pregnancies with Preeclampsia or Fetal Growth Restriction

We first sought to localise the side-population markers to a distinct trophoblast population in human placental samples via mIF. Initially, each antibody was optimised individually prior to the combination staining mIF. Opal staining evaluating co-expression of markers on a specific cell type, such as the side-population, required the selection of fluorophores that had minimal spectral overlap (Opal™ 520, Opal™ 570 and Opal™ 690). Therefore, a maximum of 3 markers plus a DAPI nuclear counterstain could be localised to any one section. Given the limited specificity of the ELL2 and GATA6 antibodies trialled (data not shown), these were not included in the two panels.

For panel 1 (Fig. 1A–J), in placentas obtained from preterm control, HLA-DPB1 positivity (Fig. 1B & G) was observed in the membrane of stromal immune cells and select trophoblasts lining the borders of villous cross sections. UPP1 (Fig. 1C & H) and SERPINE3 (Fig. 1D & I) localised to the cytoplasm of trophoblasts lining the basement membrane of the placental villi. Similar expression for each marker in panel 1 was observed in each experimental group. In panel 2 (Fig. 1K–T), each marker also demonstrated consistent localisation across all experimental groups. CXCL8 (Fig. 1L & Q) was expressed in the villous cross section in addition to syncytiotrophoblast and select underlying trophoblast layers. INTS6 (Fig. 1M & R) was localised to the nuclei of villous syncytiotrophoblast and underlying cytotrophoblast. INTS6 was also observed in the stroma and endothelial cells lining the placental vasculature (data not shown). HK2 (Fig. 1N & S) appeared to localise to the cytoplasm of similar cell populations to INTS6.

Positivity for both immunofluorescent side-population panels appeared to be specific to select trophoblasts positioned along the basement membrane of the placental villous cross sections. This was observed in the gestation-matched preterm controls. Panel 1 (HLA-DPB1 +/UPP1 +/SERPINE3 +) positivity suggested staining in suspected syncytial knots (Fig. 1E raw, J analysis), but the ability to trace these sections serially with panel 2 (INTS6 +/CXCL8 +/HK2 +) indicated that these were likely false

knots that instead reflect syncytial branching points or intervillous bridges (connection points of the syncytioplasms between neighbouring villi) (Fig. 1O raw, T analysis) [34, 35].

In placentas obtained from patients with preeclampsia (Fig. 2) or fetal growth restriction (Fig. 3) ( $n=3$  each group), mIF positivity for co-localisation of the trophoblast side-population markers was also performed. In both sets, as similarly observed to control placentas (Fig. 1), the panels of trophoblast side-population markers were only localised to select trophoblasts that bordered the basement membrane of the placental villi. There were no statistically significant changes to the cell count of cells that were positive for all assayed side-population markers (Supplementary Table I).

### Single-cell RNA Sequencing (scRNA-seq) in an Organoid Model of Trophoblast Differentiation

To gain further insight in localising the side-population panel to point/s in trophoblast differentiation, expression of each gene was assessed in a publicly available single-cell RNA sequencing (scRNA-seq) dataset [15]. This dataset originated from  $n=3$  three-dimensional hTSC-derived organoids that were treated under hTSC conditions or induced to differentiate into EVT. Processing of the single-cell RNA-sequencing data set resulted in 6354 cells that passed initial quality control. Cells were clustered in a uniform manifold approximation and projection (UMAP) plot according to transcriptionally similar states [36]. Transcriptionally similar cells and clusters were observed to be graphically closer in distance for undifferentiated (Fig. 4A) and EVT media-conditioned cultures (Fig. 4C). Each cluster was annotated with one of the following 6 cell identities: mononuclear trophoblast (MNT), proliferative mononuclear trophoblast (pMNT), pre-fusion mononuclear trophoblast (MNTpf), progenitor EVT (pEVT), invasive EVT (iEVT) and syncytiotrophoblasts (STB).

As a full panel, the 8 trophoblast side-population-enriched genes localised to most cells within undifferentiated organoid culture, (Fig. 4A–B, G) with dense expression mapping to cell identities including mononuclear trophoblasts, progenitor EVTs, invasive EVTs, and syncytiotrophoblasts. In contrast, in EVT differentiation conditions (Fig. 4C–D, H), these genes were enriched in a subset of cells undergoing syncytiotrophoblast differentiation (pre-fusion mononuclear trophoblasts and syncytiotrophoblasts), and in mononuclear trophoblasts.

Analysis localised each side-population gene to defined cell identities. *CXCL8* (*IL8*) expression was restricted to select pre-fusion mononuclear trophoblasts in undifferentiated, and syncytiotrophoblasts in differentiated cell culture (Fig. 4E–F). *ELL2* was predominantly expressed in cell

# Preterm Control

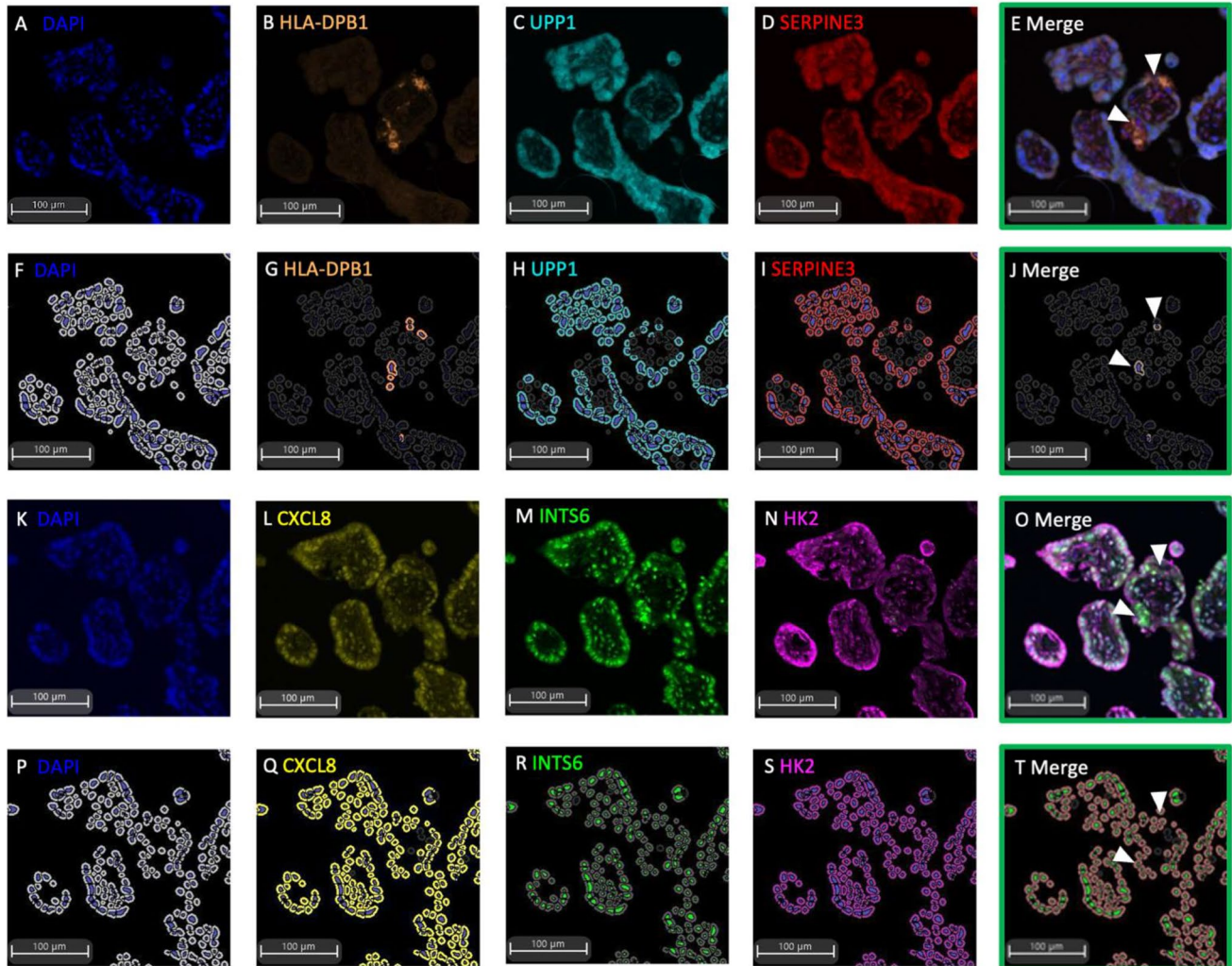


**Fig. 1** Multiplexed immunofluorescence of trophoblast side-population markers in preterm placental serial sections (<34-week gestation). One serial section stained for each of Panel 1 and 2. Representative raw images of Panel 1: DAPI nuclear counterstain (A), HLA-DPB1 (B), UPP1 (C), SERPINE3 (D), with merge of Panel 1 (E). HALO Analysis of positive immunostaining for DAPI (F), HLA-DPB1 (G), UPP1 (H), SERPINE3 (I), and cells expressing

co-localisation of Panel 1 markers (J). Representative raw images of Panel 2: DAPI counterstain (K), CXCL8 (L), INTS6 (M), HK2 (N), merge of Panel 2 (O). HALO analysis of positive immunostaining for DAPI (P), CXCL8 (Q), INTS6 (R), HK2 (S), and cells expressing co-localisation of Panel 2 markers (T). Representative images of  $n=3$  at  $10\times$  magnification shown

fusion-related identities (syncytiotrophoblast, pre-fusion mononuclear trophoblasts) under both conditions. Additional expression was observed in progenitor EVT in undifferentiated hTSC-derived organoids. *GATA6* was expressed in subsets of progenitor EVTs, mononuclear trophoblasts and proliferative mononuclear trophoblasts across culture conditions. *GATA6* was also enriched in some pre-fusion mononuclear trophoblasts. *HK2* was expressed in progenitor EVTs under both states. Further expression in undifferentiated organoid culture was limited to select invasive EVTs,

while expression was also observed in syncytiotrophoblast trajectories under EVT culture conditions (pre-fusion mononuclear trophoblasts and syncytiotrophoblasts). *HLA-DPB1* was expressed only in low numbers of invasive EVTs in both culture conditions. *INTS6* was surprisingly enriched in both culture conditions in cells associated with EVT differentiation (progenitor EVTs, invasive EVTs). *INTS6* also mapped to a subset of pre-fusion mononuclear trophoblasts in undifferentiated, and mononuclear trophoblasts in differentiated culture conditions. *SERPINE3* had enrichment in



# Preeclampsia

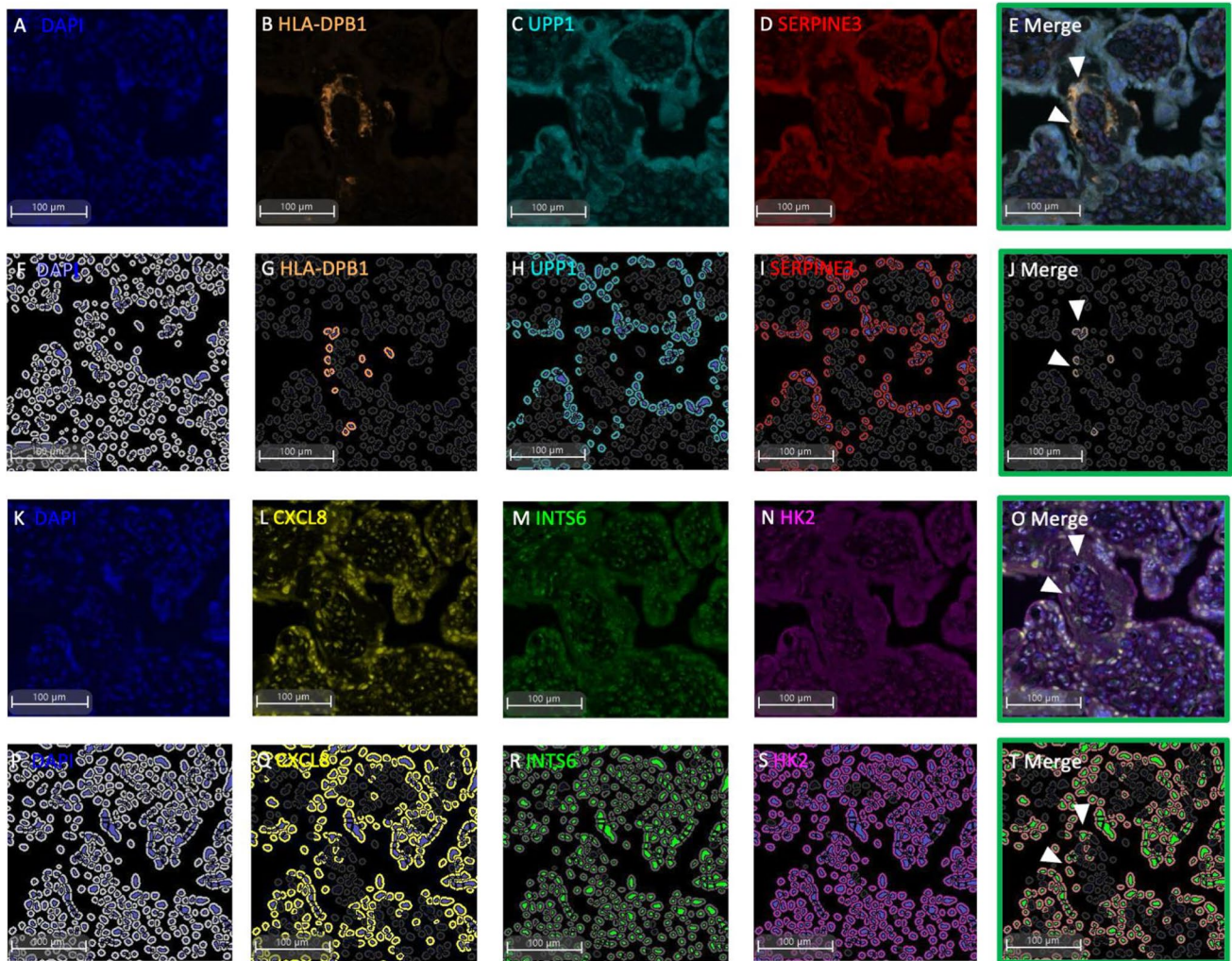


**Fig. 2** Multiplexed immunohistochemistry of trophoblast side-population markers in placentas from preterm preeclampsia (<34-week gestation). One serial section stained for each of Panel 1 and 2. Representative raw images of Panel 1: DAPI nuclear counterstain (**A**), HLA-DPB1 (**B**), UPP1 (**C**), SERPINE3 (**D**), with merge of Panel 1 (**E**). HALO Analysis of positive immunostaining for DAPI (**F**), HLA-DPB1 (**G**), UPP1 (**H**), SERPINE3 (**I**), and cells expressing

co-localisation of Panel 1 markers (**J**). Representative raw images of Panel 2: DAPI counterstain (**K**), CXCL8 (**L**), INTS6 (**M**), HK2 (**N**), merge of Panel 2 (**O**). HALO analysis of positive immunostaining for DAPI (**P**), CXCL8 (**Q**), INTS6 (**R**), HK2 (**S**), and cells expressing co-localisation of Panel 2 markers (**T**). Representative images of  $n=3$  at  $10\times$  magnification shown

select progenitor EVT and mononuclear trophoblasts, with additional expression in select undifferentiated proliferative mononuclear trophoblasts and differentiated syncytiotrophoblasts. *UPP1* expression was abundant in mononuclear trophoblasts and syncytiotrophoblasts across both groups, in undifferentiated EVT-related cell identities (progenitor EVT and invasive EVT), and finally in differentiated cell identity pre-fusion syncytiotrophoblasts.

## Trophoblast Side-population Gene Expression in Human Trophoblast Stem Cell (hTSC) Differentiation to Extravillous Trophoblast and Syncytiotrophoblast Phenotypes

To validate findings in scRNA-seq, we measured side-population marker mRNA expression in an *in vitro* model of trophoblast differentiation using hTSCs [30]. The timepoints

## Fetal Growth Restriction

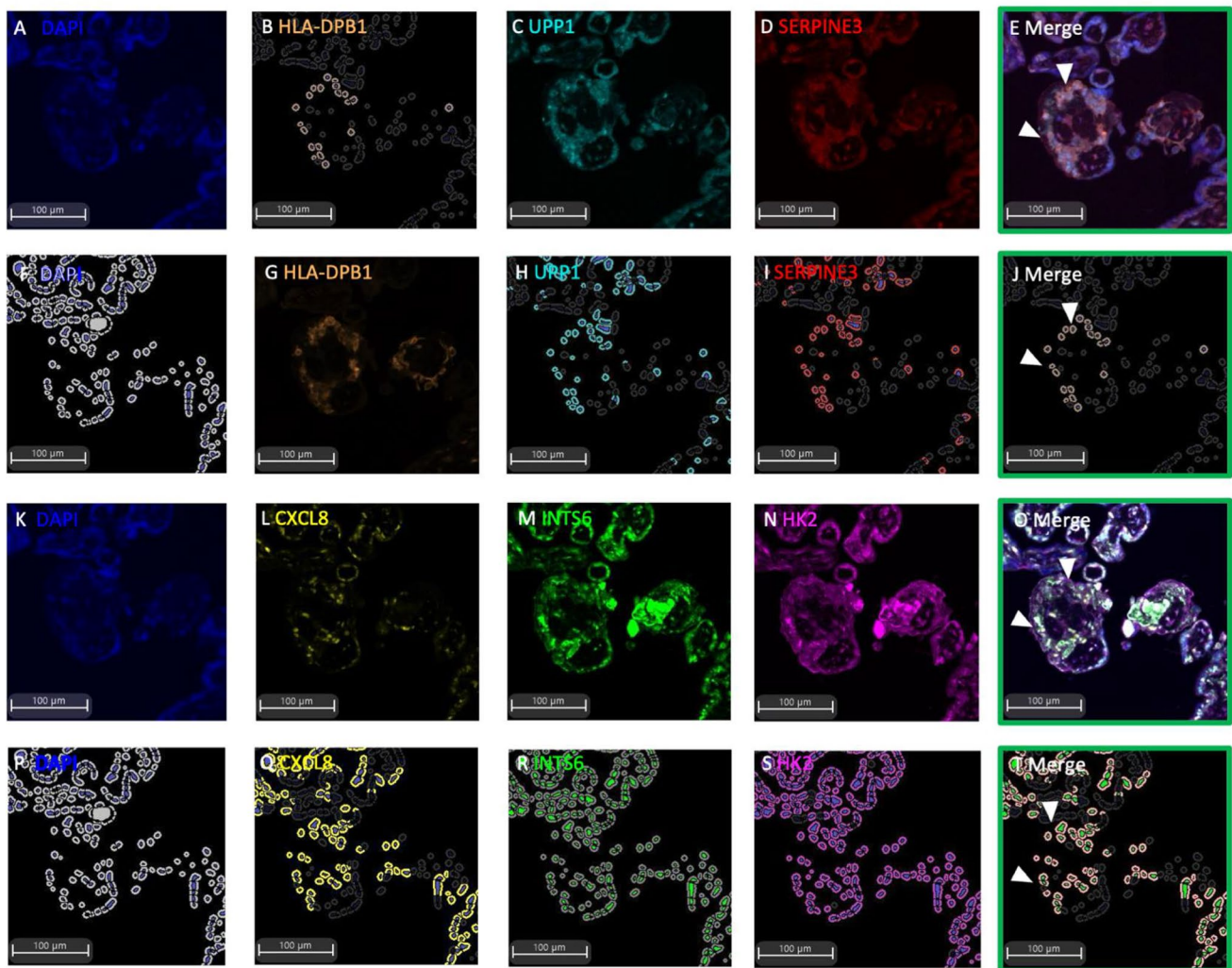


**Fig. 3** Multiplexed immunohistochemistry of trophoblast side-population markers in placentas from fetal growth restriction (<34-week gestation). One serial section stained for each of Panel 1 and 2. Representative raw images of Panel 1: DAPI nuclear counterstain (A), HLA-DPB1 (B), UPP1 (C), SERPINE3 (D), with merge of Panel 1 (E). HALO Analysis of positive immunostaining for DAPI (F), HLA-DPB1 (G), UPP1 (H), SERPINE3 (I), and cells expressing

co-localisation of Panel 1 markers (J). Representative raw images of Panel 2: DAPI counterstain (K), CXCL8 (L), INTS6 (M), HK2 (N), merge of Panel 2 (O). HALO analysis of positive immunostaining for DAPI (P), CXCL8 (Q), INTS6 (R), HK2 (S), and cells expressing co-localisation of Panel 2 markers (T). Representative images of  $n=3$  at  $10\times$  magnification shown

examined were 0, 48 and 96 h post-differentiation in to the two main trophoblast lineages: extravillous trophoblasts (EVTs) and syncytiotrophoblasts.

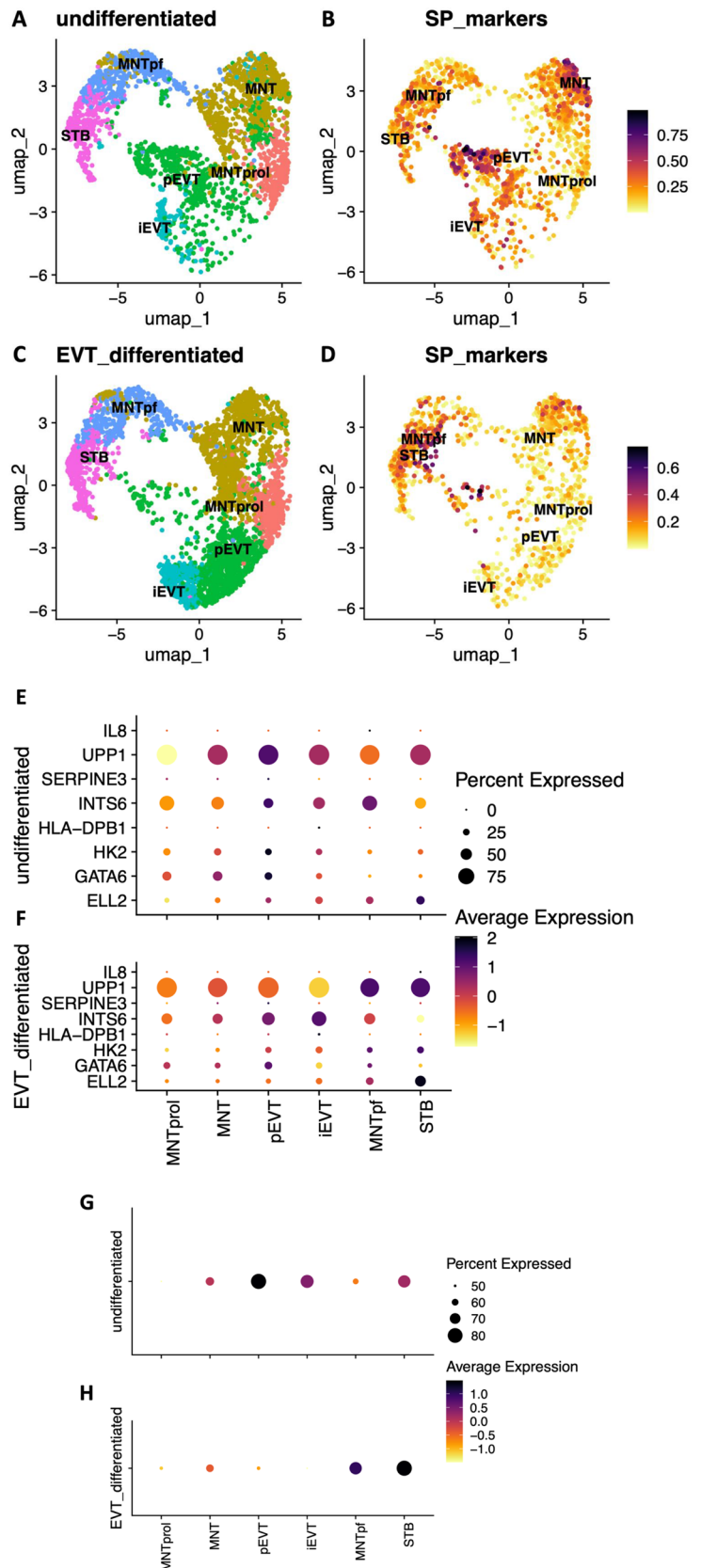
Successful EVT differentiation was confirmed morphologically and via loss of the hTSC marker, *TEAD4* (Fig. 5A,  $p=0.0067$  at 72 h,  $p=0.0018$  at 96 h) and increases to EVT marker *HLA-G* (Fig. 5B,  $p=0.026$  at 72 h,  $p=0.0002$  at 96 h). *CXCL8* reduced briefly with EVT differentiation (Fig. 5C,  $p=0.030$  at 48 h post-differentiation). Meanwhile, *ELL2* (Fig. 5D,  $p=0.0047$  at 96 h), *GATA6* (Fig. 5E,  $p=0.0039$  96 h), and *HK2* (Fig. 5F,

$p=0.018$  at 72 h,  $p=0.0003$  at 96 h) increased with differentiation to EVT. Conversely, *HLA-DPB1* expression was reduced (Fig. 5G,  $p=0.011$  at 48 h,  $p=0.0046$  at 72 h). *INTS6* was additionally upregulated with EVT differentiation (Fig. 5H,  $p=0.0092$  at 72 h,  $p=0.0005$  at 96 h). *UPP1* was unaltered with EVT differentiation (Fig. 5I), and *SERPINE3* expression was undetectable at all timepoints.

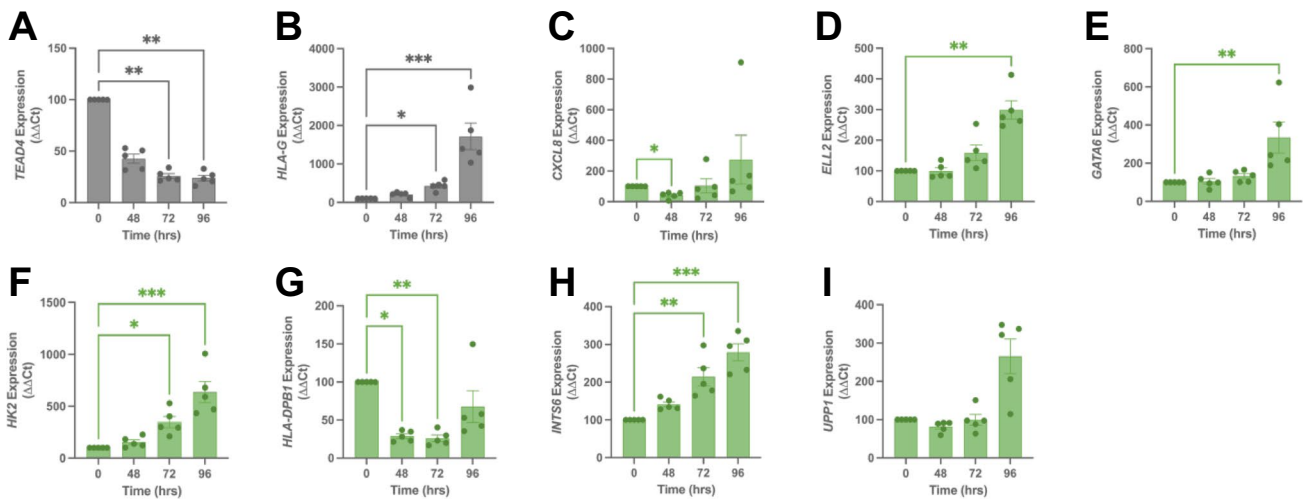
Syncytialisation was confirmed morphologically, and via loss of *TEAD4* expression (Fig. 5J,  $p=0.0006$  at 96 h) coupled with raised syncytiotrophoblast marker *SDC1* expression



**Fig. 4** Single-cell RNA sequencing analysis of the trophoblast side-population-enriched genes in human trophoblast stem cell (hTSC) organoids and differentiated extravillous trophoblasts (EVTs). Transcriptomic analysis of a publicly available single-cell RNA sequencing dataset of  $n = 3$  biological replicates of three-dimensional hTSC-derived organoids treated under hTSC conditions or induced to differentiate to EVT for 21 days (Shannon et al., *Development* 2022). Analysis resulted in 6 distinct transcriptomic cell identities: mononuclear trophoblast (MNT), proliferative mononuclear trophoblast (MNTprol), pre-fusion mononuclear trophoblast (MNTpf), progenitor EVT (pEVT), invasive EVT (iEVT) and syncytiotrophoblast (STB). UMAP plot of cell identities in undifferentiated hTSC organoids (A). Feature plot showing a module score analysis for trophoblast side-population genes *CXCL8* (*IL8*), *ELL2*, *GATA6*, *HK2*, *HLA-DPB1*, *INTS6*, *SERPINE3*, and *UPP1* where the relative expression of these genes is plotted (B). UMAP plot of cell identities in differentiated EVT organoid culture (C). A feature plot showing a module score analysis for trophoblast side-population genes in EVT organoid culture (D). Dot plot of each trophoblast-side population marker gene expression to specific cell identities in undifferentiated (E) and differentiated EVT (F) organoid culture. Dot plot of the module scores for all trophoblast side-population panel markers in undifferentiated (G) and differentiated (H) organoid culture



## Extravillous trophoblast differentiation



## Syncytiotrophoblast differentiation

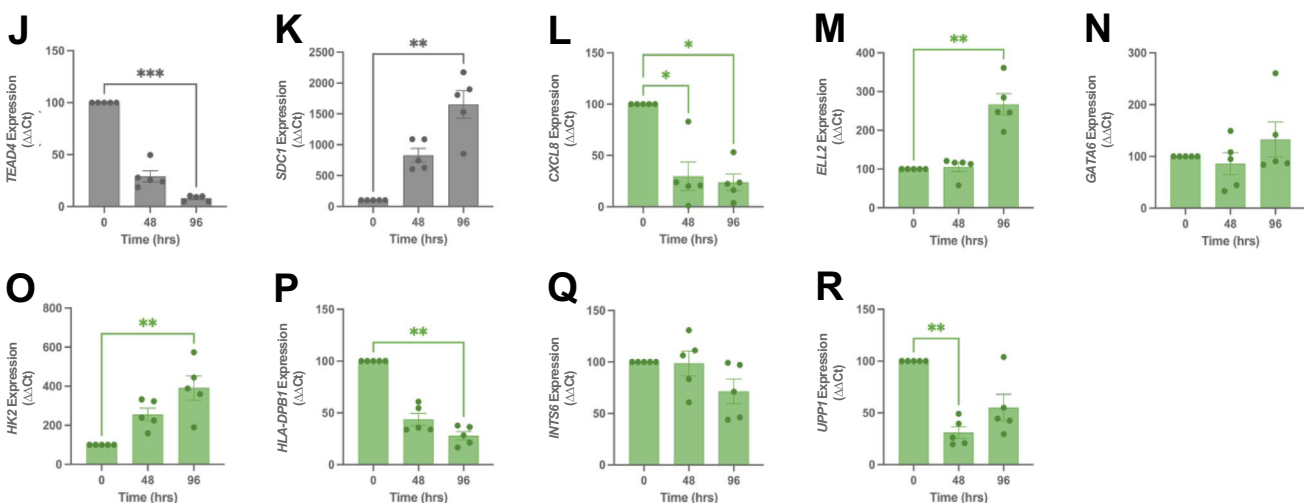


**Fig. 5** Trophoblast side-population-enriched genes and their expression with differentiation of human trophoblast stem cells (hTSCs) to extravillous trophoblasts and syncytiotrophoblasts. hTSCs were differentiated to extravillous trophoblasts (EVT) at 0, 48, 72 and 96 h post-differentiation, or syncytiotrophoblasts at 0, 48, 96 h post-differentiation. EVT differentiation was confirmed with *TEAD4* loss ( $p=0.0067$  72 h,  $p=0.0018$  96 h) (A) and induction of *HLA-G* expression ( $p=0.026$  72 h,  $p=0.0002$  96 h) (B). As hTSCs differentiated to EVTs, *CXCL8* expression was reduced ( $p=0.030$ ) (C). *ELL2* ( $p=0.0047$ ) (D), *GATA6* ( $p=0.0039$ ) (E) and *HK2* ( $p=0.018$  72 h,  $0.0003$  96 h) (F) were upregulated. *HLA-DPBI* expression reduced ( $p=0.011$  48 h,  $p=0.0046$  72 h) (G). *INTS6* was upregulated ( $p=0.0092$  72 h,  $p=0.0005$  96 h) (H). *UPP1* was unaltered

(I). *SERPINE3* was not expressed at any timepoint (data not shown). Syncytiotrophoblast differentiation was confirmed with *TEAD4* loss ( $p=0.0006$ ) (J) and *SDC1* gain ( $p=0.0011$ ) (K). As hTSCs differentiated to syncytiotrophoblasts, *CXCL8* was reduced ( $p=0.015$  48 h,  $p=0.012$  96 h) (L). *ELL2* was upregulated ( $p=0.0024$  96 h) (M), *GATA6* was unaltered (N), *HK2* was raised ( $p=0.0019$ ) (O), *HLA-DPBI* was reduced at 48 h (with low statistical significance  $p=0.051$ ) and 96 h ( $p=0.0031$ ) (P). *INTS6* was unaltered (Q). *UPP1* expression was downregulated ( $p=0.0063$ ) (R). mRNA expression was normalised to the geometric mean of housekeeper genes. Data expressed as mean  $\pm$  SEM with all experiments repeated  $n=5$  in triplicates for EVTs and duplicates for syncytiotrophoblasts. \* $p<0.05$ , \*\* $p<0.01$ , \*\*\* $p<0.001$

(Fig. 5K,  $p=0.0011$  at 96 h). While *CXCL8* reduced with differentiation (Fig. 5L,  $p=0.015$  at 48 h,  $p=0.012$  at 96 h), *ELL2* was upregulated (Fig. 5M,  $p=0.0024$  at 96 h), and *GATA6* was unaltered (Fig. 5N). *HK2* expression increased (Fig. 5O,  $p=0.0019$  at 96 h). *HLA-DPBI* was reduced at 48 h

but did not hold statistical significance (Fig. 5P,  $p=0.051$ ) until 96 h post-differentiation ( $p=0.0031$ ). *INTS6* was unaltered (Fig. 5Q). Finally, *UPP1* was downregulated (Fig. 5R,  $p=0.0063$  at 48 h), while *SERPINE3* expression was also undetectable at all timepoints with syncytialisation.

## Trophoblast Side-population Gene Expression in Preeclampsia and Fetal Growth Restriction

Placental mRNA expression was examined for the 8 genes enriched in isolated trophoblast side-population cells (*CXCL8/IL8*, *ELL2*, *GATA6*, *HK2*, *HLA-DPBI*, *INTS6*, *SERPINE3*, *UPPI*) in placentas obtained from participants with early onset preeclampsia ( $n = 78$ ) or fetal growth restriction ( $n = 30$ ). Expression was compared to gestation-matched controls ( $n = 18$ ). All genes were expressed in the placental samples. Of the 8 trophoblast side-population genes, *CXCL8* (Fig. 6A,  $p = 0.0335$  in preeclampsia; Fig. 6B,  $p = 0.0001$  in FGR) and *ELL2* (Fig. 6C,  $p = 0.0006$ ; Fig. 6D,  $p = 0.0065$  respectively) were upregulated. *GATA6* was downregulated in preeclampsia (Fig. 6E,  $p = 0.0014$ ) and FGR (Fig. 6F,  $p = 0.0146$ ). *HK2* was significantly upregulated in both conditions (Fig. 6G preeclampsia, Fig. 6H in FGR,  $p < 0.0001$  both conditions). The remaining 4 genes were unaltered in both preeclamptic and FGR placentas (*HLA-DPBI*, Fig. 6I-J; *INTS6*, Fig. 6K-L; *SERPINE3*, Fig. 6M-N; and *UPPI*, Fig. 6O-P).

Placentas affected by concurrent preeclampsia and fetal growth restriction were included in each disease cohort. Thus, we also examined differences between those with one complication (only preeclampsia or only FGR) or both (concurrent preeclampsia and FGR) relative to controls (Supplementary Fig. 1). When stratified, *CXCL8* expression remained elevated in placentas obtained from FGR pregnancies, irrespective of concurrent preeclampsia (Supplementary Fig. 1A,  $p = 0.0003$  FGR,  $p = 0.0033$  FGR/preeclampsia). Conversely, no change was observed in those with preeclampsia alone. *ELL2* was unaltered in placentas from deliveries with FGR only. Its expression was elevated in the placenta from preeclamptic pregnancies, regardless of simultaneous FGR (Supplementary Fig. 1B,  $p = 0.0004$  preeclampsia,  $p = 0.0023$  FGR/preeclampsia). *GATA6* expression was reduced in placentas obtained from preeclamptic pregnancies, and in those that also delivered with FGR (Supplementary Fig. 1C,  $p = 0.0014$  preeclampsia,  $p = 0.015$  FGR/preeclampsia). Increased *HK2* was observed in all diseased groups but was most pronounced in placentas obtained from pregnancies complicated by preeclampsia (Supplementary Fig. 1D, FGR  $p = 0.015$ , FGR/preeclampsia  $p = < 0.0001$ , preeclampsia  $p < 0.0001$ ). While unaltered statistically in placentas from pregnancies complicated by FGR in initial analysis, when stratified, *INTS6* was markedly reduced ( $p < 0.0001$ ), specifically in placentas affected by FGR alone. It remained unaltered in samples from FGR/preeclampsia and preeclampsia only (Supplementary Fig. 1F). *SERPINE3* and *UPPI* (Supplementary Fig. 1G, Supplementary Fig. 1H respectively) remained unaltered across each stratified disease cohort.

## Discussion

In this study, we sought to localise the 8 genes enriched in trophoblast side-population cells in the human placenta and characterise their expression in placental insufficiency. When analysed as individual genes, expression was induced following differentiation to EVT or syncytiotrophoblasts. However, the power of the panel lies in the combined analysis. We visualised 6 of the 8 trophoblast side-population markers using multiplexed immunofluorescence, revealing localisation is likely restricted to rare trophoblast sub-populations, where contiguous villi may intersect. Analysis of single-cell sequencing data confirmed co-localisation of trophoblast side-population genes to a mononuclear trophoblast identity. Furthermore, of the 8 genes, 5 of them: *CXCL8*, *ELL2*, *GATA6* and *HK2*, and *INTS6* were found to be dysregulated in placenta obtained from pregnancies complicated by placental insufficiency.

We found that side-population markers were co-expressed in distinct trophoblast sub-types lining the basement membrane of the placental villi. These findings concur with current understanding of the residence of isolated human trophoblast stem cells [37]. In both disorders, dysregulated progenitor trophoblasts may contribute to homeostatic dysfunction, thereby initiating trajectories towards programmed cell death (apoptosis) [38]. Further insults to progenitor trophoblasts may impair differentiation processes. Downstream ramifications to effector functions may include villous formation and function [39]. Indeed, development of immature and aberrant placental villi that eventuate to a poorly perfused placenta and an impeded ability to perform as a specialised maternal-fetal interface has previously been identified [40, 41]. The current study identified a potential side-population of trophoblast cells localised to specific regions within the placental villi. Taken together with the transcriptomic analysis demonstrating enrichment in mononuclear trophoblast sub-types, this work may provide insight on the relevance of these cells and to how these processes may be disrupted in placental insufficiency. Future studies should importantly embark upon histological analysis beyond the villi that includes the anchoring columns where EVT differentiation occurs.

The side-population method results in a purified isolation of what are proposed to include trophoblasts higher in the lineage hierarchy, including trophoblast stem cells [42]. Isolation of side-population trophoblasts alongside cytotrophoblast isolation was recently used to generate organoids [43], providing a valuable tool to recapitulate the *in vivo* microenvironment of trophoblast stem cells more closely. Side-population cells are enriched in cancer stem cell populations and confer drug resistance to chemotherapeutics in other reproductive contexts including endometrial and breast



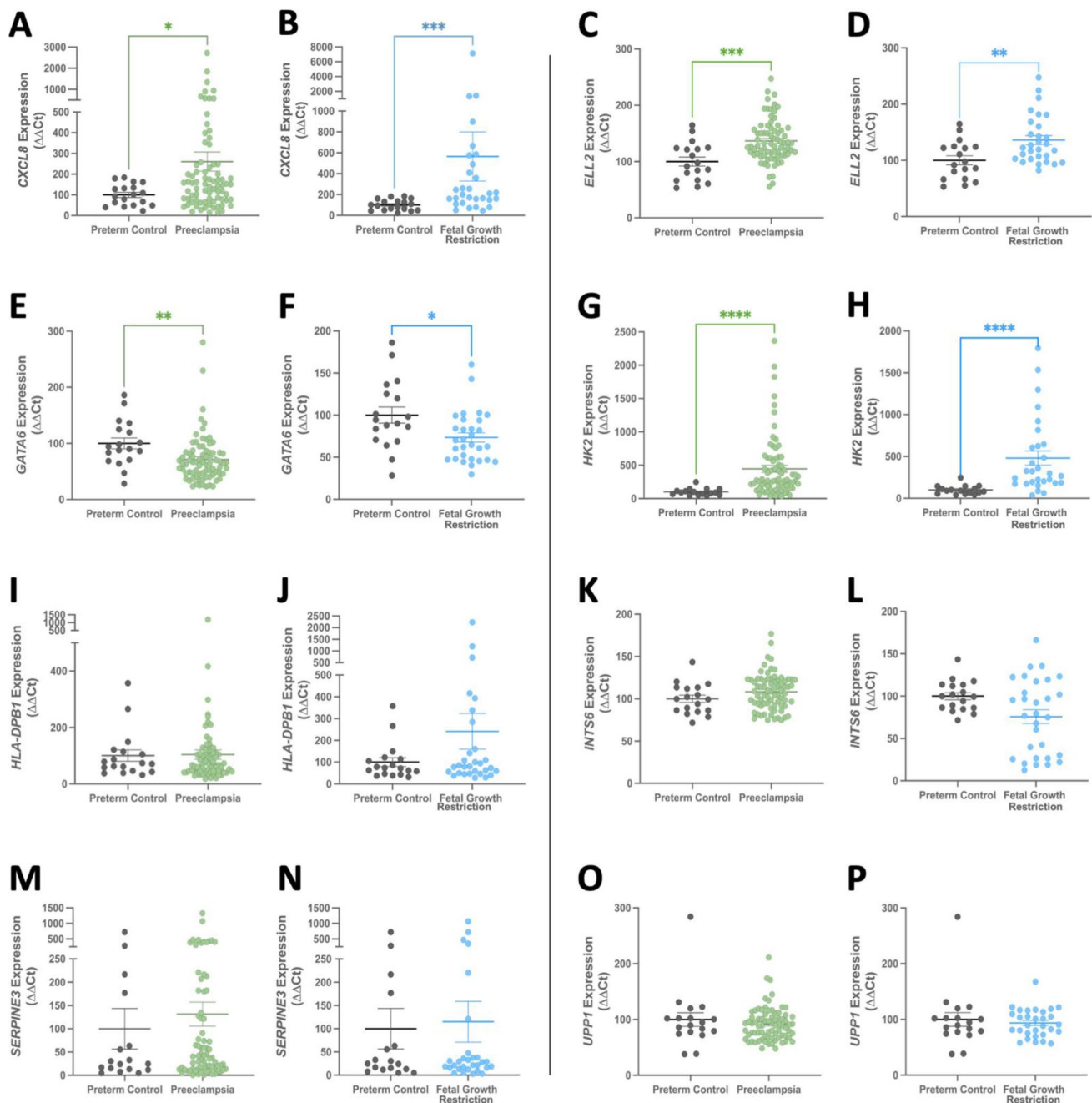


**Fig. 6** Trophoblast side-population-enriched genes *CXCL8*, *ELL2*, *GATA6*, and *HK2* are dysregulated in placentas obtained from pregnancies complicated by preeclampsia and fetal growth restriction. mRNA expression of side-population genes in placentas from participants with preeclampsia ( $n=78$  green circle), or fetal growth restriction (FGR,  $n=30$ , blue circle) compared to gestation-matched preterm ( $<34$ -week) controls ( $n=18$ , grey circle). *CXCL8* was upregulated in preeclampsia ( $p=0.037$ ) (A) and FGR ( $p=0.0001$ ) (B). *ELL2* was elevated in preeclampsia ( $p=0.0006$ ) (C) and FGR ( $p=0.0065$ ) (D). *GATA6* was downregulated in preeclampsia

( $p=0.0014$ ) (E) and FGR ( $p=0.0146$ ) (F). *HK2* was upregulated in preeclampsia ( $p<0.0001$ ) (G) and FGR ( $p<0.0001$ ) (H). *HLA-DPB1* was unaltered in preeclampsia (I) and FGR (J); as was *INTS6* in preeclampsia (K) and FGR (L); *SERPINE3* in preeclampsia (M) and FGR (N); and *UPP1* in preeclampsia (O) and FGR (P). mRNA expression was normalised to the geometric mean of housekeeper genes. Individual symbols represent individual participants. Data is expressed as mean  $\pm$  SEM. \* $p<0.05$ , \*\* $p<0.01$ , \*\*\* $p<0.001$ , \*\*\*\* $p<0.0001$

cancer [44–46]. Investigating trophoblast side-population cells may therefore provide insights into their response to therapeutics, and interventions for placental insufficiency. Whilst the side-population method results in a more purified isolation of stem cells, it inevitably yields a heterogeneous progenitor cell population [10]. This is reflected in the heterogeneous cell type enrichment for side-population genes in our transcriptomic data. These findings emphasise that following studies must continue to interrogate the molecular governance of trophoblast stem cells that may be relevant to placental insufficiency pathogenesis. It would be intriguing to identify whether these 8 markers reflect the full spectrum or a unique subset [47] of a side-population trophoblast isolation, and then which subset, if any, contributes to placental insufficiency disorders.

While CXCL8 is a classical proinflammatory cytokine, it also has roles in stem cell activity in response to senescent microenvironments [48, 49]. Indeed, placental ageing is considered a pathogenic mechanism of placental insufficiency [2, 50, 51]. In the placenta, CXCL8 may be involved in trophoblast migration, proliferation, and invasion [52–54]. The elevated CXCL8 observed in placentas obtained from FGR deliveries may indicate disruptions to these processes in a trophoblast side-population. CXCL8 has previously shown to be raised in placentas of participants with established preeclampsia, with exacerbations in severe disease [55, 56]. Given minute expression in hTSC and EVT-related differentiation trajectories, and diffuse expression observed in immunofluorescent staining and hTSC *in vitro* differentiation studies, CXCL8 expression alone is likely not restricted to a specific placental cell type. It may therefore play multiple roles within the placenta.

*ELL2* encodes for a component of transcription elongation [57]. In our findings, *ELL2* expression was upregulated in placentas with established disease compared to their gestation-matched counterparts. Moreover, *ELL2* was downregulated in first trimester placentas obtained from chorionic villous sampling preceding a preeclampsia diagnosis [58]. The placenta-specific functions of *ELL2* remain poorly understood [59]. It may inhibit wntless-related integration site (WNT) signalling, a key molecular pathway that directs progenitor function in the placenta and other processes in placental development [60]. In this study, *ELL2* and *GATA6* were unable to be localised as the Opal multiplexed immunofluorescence method was restricted to a maximum of 3 markers co-localised to any one cell in addition to DAPI nuclear counterstaining, with each representing a different subcellular compartment. Furthermore, the commercial antibodies available for these two markers displayed limited antibody specificity in the optimisation process.

The reduction in *GATA6* expression that appeared specific to preeclampsia provides a novel finding, as it has yet to be explored in the placenta or in pregnancy. In the intestine,

where *GATA6* is better characterised, *GATA6* activates intestinal caudal type homeobox 2 (*CDX2*) expression. Here, it directs commitment to differentiation to the intestinal epithelial cell types and is dysregulated in gastrointestinal adenocarcinomas [61, 62]. In the placenta, *CDX2* is involved in trophoblast fate specification, and is instrumental to the maintenance of trophoblast stem cell populations [30, 63]. *GATA6* may therefore have analogous placental roles to its intestinal function. Observed reductions to *GATA6* expression in preeclampsia and enrichment in trophoblasts committed to an EVT cell fate may therefore indicate aberrations in trophoblast specification.

This study demonstrated that placental *HK2* is elevated in both FGR and preeclampsia, with elevated expression in trophoblasts that have likely undergone a cell fate commitment. *HK2* is a crucial glycolysis enzyme, and tightly regulates its balance with cell autophagy [64]. Intriguingly, *HK2* activity itself is inhibited in a hypoxic environment. It may be important in the altered oxygen tension states in early pregnancy [65]. By extension, it may reflect compensatory mechanisms in response to the hypoxia and cell turnover observed in placental insufficiency disorders such as preeclampsia [66]. There have been confounding results in the field as to the direction of altered *HK2* expression in preeclampsia, with most findings observed in decidual tissue [60, 67–69]. *HK2* activity is heightened with metabolic stress and maintains cancer stem cell potency [70]. The link between *HK2* and trophoblast stem cell potency or response to environmental stress may be an interesting point for further research.

Until now, *INTS6* expression has not yet been explored in the placenta. Our findings show that *INTS6* expression is reduced exclusively in FGR. While FGR and preeclampsia share many pathophysiological aspects, the molecular governance of these processes has points of divergence. *INTS6* is more enriched in cells that have differentiated to terminal trophoblast phenotypes. *INTS6* is known to inhibit proliferation via the WNT, protein kinase B (*AKT*) and extracellular signal-related kinase (*ERK*) signalling pathways [71–73]. Given that these pathways are also active in the placenta, *INTS6* may function similarly here too. Reduced *INTS6* expression may therefore contribute to reduced cytotrophoblast proliferation that may occur in FGR [74].

Further steps beyond this study could be to isolate trophoblasts based on enrichment of trophoblast side-population markers, and to test whether they function similarly to the original trophoblast side-population isolated through the Hoechst method. Centrifugation speed, which may aid in purified isolation of potentially small-sized resident trophoblast stem cells, should be considered in these studies [75, 76]. Validating transcriptomic data with *in vitro* and *in vivo* experimentation would also be key to interpreting and furthering our understanding of mechanisms critical to trophoblast function, in both placental development and disease.

## Conclusion

We have limited understanding of each side-population marker in the placenta, and in placental insufficiency. This study identified the potential location of a unique trophoblast subset that is enriched for side-population markers. Furthermore, while each side-population marker alone may not be sufficient to determine progenitor function, it is important that all markers are considered collectively as a panel in future in depth functional studies. These findings contribute to the hypothesis that the trophoblast subtype indicated by side-population markers may represent a specific trophoblast identity that functions differentially to other trophoblast populations, and when dysregulated gives rise to placental insufficiency that leads to disorders of pregnancy including preeclampsia and/or FGR.

**Supplementary Information** The online version contains supplementary material available at <https://doi.org/10.1007/s12015-024-10764-w>.

**Acknowledgements** The authors would like to acknowledge research midwives Kaitlin Constable, Melissa Sutton, Gabrielle Pell, Genevieve Christophers, Rachel Murdoch, Alison Abboud, the clinical staff, and patients at the Mercy Hospital for Women (Heidelberg) for the provision of samples used in this work. We also thank the pathology, health information services, and antenatal clinic staff at the Mercy Hospital for Women in their assistance in conducting this research. First trimester trophoblast stem cells were obtained from the RIKEN BRC through the National BioResource Project of the MEXT/AMED, Japan.

**Author Contributions** Conceptualization, G.P.W. and T.J.K.-L.; Methodology, G.P.W., S.E., P.C., T.-V.N., A.N., L.A.B., N.J.H., D.G.S. and T.J.K.-L.; Formal Analysis, G.P.W., S.H., S.E., and O.N.; Investigation, G.P.W. and T.K.L.; Resources, T.J.K.-L., N.J.H., S.T., Writing – Original Draft Preparation, G.P.W., T.J.K.-L.; Writing – Review and Editing, all authors; Supervision, T.J.K.-L., N.J.H., and D.G.S.; Funding Acquisition, T.J.K.-L., S.T., D.G.S. All authors have read and agreed to the final version of the manuscript.

**Funding** Open Access funding enabled and organized by CAUL and its Member Institutions. Salary support was provided by the Australian Research Council Fellowships to N.J.H. (#FT10100193) and T.K.L. (#FT230100125), and National Health and Medical Research Council Fellowship to S.T. (#2017897). The funders played no role in study design or analysis.

**Data Availability** All data from this study are available within the publication and supplementary files. Other resources used in this study are available from the corresponding author upon reasonable request. The full code used for single-cell transcriptomics is available upon request.

## Declarations

**Ethics Approval and Consent to Participate** Placental samples were sourced from the Mercy Hospital for Women Tissue Bank (Heidelberg, Victoria, Australia). Samples were donated following informed, written consent. This study was approved by the Mercy Health Human Research Ethics Committee (R11/34).

**Consent for Publication** All authors have read and approved this publication.

**Conflicts of Interest** The authors declare no conflicts of interest nor competing interests.

**Open Access** This article is licensed under a Creative Commons Attribution 4.0 International License, which permits use, sharing, adaptation, distribution and reproduction in any medium or format, as long as you give appropriate credit to the original author(s) and the source, provide a link to the Creative Commons licence, and indicate if changes were made. The images or other third party material in this article are included in the article's Creative Commons licence, unless indicated otherwise in a credit line to the material. If material is not included in the article's Creative Commons licence and your intended use is not permitted by statutory regulation or exceeds the permitted use, you will need to obtain permission directly from the copyright holder. To view a copy of this licence, visit <http://creativecommons.org/licenses/by/4.0/>.

## References

- Abalos, E., Cuesta, C., Grosso, A. L., Chou, D., & Say, L. (2013). Global and regional estimates of preeclampsia and eclampsia: A systematic review. *European Journal of Obstetrics & Gynecology and Reproductive Biology*, *170*(1), 1–7.
- Dimitriadis, E., Rolnik, D. L., Zhou, W., Estrada-Gutierrez, G., Koga, K., Francisco, R. P. V., Whitehead, C., Hyett, J., da Silva, C. F., Nicolaides, K., & Menkhorst, E. (2023). Pre-eclampsia. *Nature Reviews Disease Primers*, *9*(1), 8.
- Gardosi, J., Madurasinghe, V., Williams, M., Malik, A., & Francis, A. (2013). Maternal and fetal risk factors for stillbirth: Population based study. *BMJ*, *24*(346), f108.
- Mustata, R. C., Van Loy, T., Lefort, A., Libert, F., Strollo, S., Vassart, G., & Garcia, M. I. (2011). Lgr4 is required for paneth cell differentiation and maintenance of intestinal stem cells ex vivo. *EMBO Reports*, *12*(6), 558–564.
- Hsu, Y. C., Li, L., & Fuchs, E. (2014). Transit-amplifying cells orchestrate stem cell activity and tissue regeneration. *Cell*, *157*(4), 935–949.
- Chang, C. W., Wakeland, A. K., & Parast, M. M. (2018). Trophoblast lineage specification, differentiation and their regulation by oxygen tension. *Journal of Endocrinology*, *236*(1), R43–R56.
- James, J. L., Boss, A. L., Sun, C., Allerkamp, H. H., & Clark, A. R. (2022). From stem cells to spiral arteries: A journey through early placental development. *Placenta*, *125*, 68–77.
- Golebiewska, A., Brons, N. H., Bjerkvig, R., & Niclou, S. P. (2011). Critical appraisal of the side population assay in stem cell and cancer stem cell research. *Cell Stem Cell*, *8*(2), 136–147.
- Goodell, M. A., Brose, K., Paradis, G., Conner, A. S., & Mulligan, R. C. (1996). Isolation and functional properties of murine hematopoietic stem cells that are replicating in vivo. *Journal of Experimental Medicine*, *183*(4), 1797–1806.
- Challen, G. A., & Little, M. H. (2006). A side order of stem cells: The sp phenotype. *Stem Cells*, *24*(1), 3–12.
- James, J. L., Hurley, D. G., Gamage, T. K., Zhang, T., Vather, R., Pantham, P., Murthi, P., & Chamley, L. W. (2015). Isolation and characterisation of a novel trophoblast side-population from first trimester placentae. *Reproduction*, *150*(5), 449–462.
- Gamage, T. K., Perry, J. J., Fan, V., Groom, K., Chamley, L. W., & James, J. L. (2020). Side-population trophoblasts exhibit the differentiation potential of a trophoblast stem cell population, persist to term, and are reduced in fetal growth restriction. *Stem Cell Reviews and Reports*, *16*(4), 764–775.



13. Quigley, L. T., Pang, L., Tavancheh, E., Ernst, M., Behren, A., Huynh, J., & Da Gama, D. J. (2023). Protocol for investigating tertiary lymphoid structures in human and murine fixed tissue sections using opal-tsa multiplex immunohistochemistry. *STAR Protocols*, 4(1), 101961.
14. VirathamPulsawatdi, A., Craig, S. G., Bingham, V., McCombe, K., Humphries, M. P., Senevirathne, S., Richman, S. D., Quirke, P., Campo, L., Domingo, E., Maughan, T. S., James, J. A., & Salto-Tellez, M. (2020). Cell trajectory modeling identifies a primitive trophoblast state defined by beam enrichment. *Molecular Oncology*, 14(10), 2384–2402.
15. Shannon, M. J., Baltayeva, J., Castellana, B., Wachter, J., McNeill, G. L., Yoon, J. S., Treissman, J., Le, H. T., Lavoie, P. M., & Berstain, A. G. (2022). Cell trajectory modeling identifies a primitive trophoblast state defined by beam enrichment. *Development*, 149(1). <https://doi.org/10.1242/dev.199840>
16. Butler, A., Hoffman, P., Smibert, P., Papalexis, E., & Satija, R. (2018). Integrating single-cell transcriptomic data across different conditions, technologies, and species. *Nature Biotechnology*, 36(5), 411–420.
17. Stuart, T., Butler, A., Hoffman, P., Hafemeister, C., Papalexis, E., Mauck, W. M., 3rd., Hao, Y., Stoeckius, M., Smibert, P., & Satija, R. (2019). Comprehensive integration of single-cell data. *Cell*, 177(7), 1888–1902 e1821.
18. McGinnis, C. S., Murrow, L. M., & Gartner, Z. J. (2019). Doublet-finder: Doublet detection in single-cell rna sequencing data using artificial nearest neighbors. *Cell Systems*, 8(4), 329–337 e324.
19. Abed, M., Verschuere, E., Budayeva, H., Liu, P., Kirkpatrick, D. S., Reja, R., Kummerfeld, S. K., Webster, J. D., Gierke, S., Reichelt, M., Anderson, K. R., Newman, R. J., Roose-Girma, M., Modrusan, Z., Pektas, H., Maltepe, E., Newton, K., & Dixit, V. M. (2019). The gag protein peg10 binds to rna and regulates trophoblast stem cell lineage specification. *PLoS ONE*, 14(4), e0214110.
20. Arutyunyan, A., Roberts, K., Troule, K., Wong, F. C. K., Sheridan, M. A., Kats, I., Garcia-Alonso, L., Velten, B., Hoo, R., Ruiz-Morales, E. R., Sancho-Serra, C., Shilts, J., Handfield, L. F., Marconato, L., Tuck, E., Gardner, L., Mazzeo, C. I., Li, Q., Kelava, I., ... Vento-Tormo, R. (2023). Spatial multiomics map of trophoblast development in early pregnancy. *Nature*, 616(7955), 143–151.
21. Li, Y., Moretto-Zita, M., Leon-Garcia, S., & Parast, M. M. (2014). P63 inhibits extravillous trophoblast migration and maintains cells in a cytotrophoblast stem cell-like state. *American Journal of Pathology*, 184(12), 3332–3343.
22. Mi, S., Lee, X., Li, X., Veldman, G. M., Finnerty, H., Racie, L., LaVallie, E., Tang, X. Y., Edouard, P., Howes, S., Keith, J. C., Jr., & McCoy, J. M. (2000). Syncytin is a captive retroviral envelope protein involved in human placental morphogenesis. *Nature*, 403(6771), 785–789.
23. Hunt, J. S., & Orr, H. T. (1992). Hla and maternal-fetal recognition. *The FASEB Journal*, 6(6), 2344–2348.
24. Isaka, K., Usuda, S., Ito, H., Sagawa, Y., Nakamura, H., Nishi, H., Suzuki, Y., Li, Y. F., & Takayama, M. (2003). Expression and activity of matrix metalloproteinase 2 and 9 in human trophoblasts. *Placenta*, 24(1), 53–64.
25. Meinhardt, G., Kaltenberger, S., Fiala, C., Knofler, M., & Pollheimer, J. (2015). Erbb2 gene amplification increases during the transition of proximal egfr(+) to distal hla-g(+) first trimester cell column trophoblasts. *Placenta*, 36(8), 803–808.
26. Chang, W. L., Liu, Y. W., Dang, Y. L., Jiang, X. X., Xu, H., Huang, X., Wang, Y. L., Wang, H., Zhu, C., Xue, L. Q., Lin, H. Y., Meng, W., & Wang, H. (2018). Plac8, a new marker for human interstitial extravillous trophoblast cells, promotes their invasion and migration. *Development*, 145(2). <https://doi.org/10.1242/dev.148932>
27. Schrey, S., Wurst, U., Ebert, T., Kralisch, S., Drewlo, S., Stepan, H., Lossner, U., Platz, M., Kratzsch, J., Stumvoll, M., & Fasshauer, M. (2015). The adipokine preadipocyte factor-1 is downregulated in preeclampsia and expressed in placenta. *Cytokine*, 75(2), 338–343.
28. Lee, C. Q., Gardner, L., Turco, M., Zhao, N., Murray, M. J., Coleman, N., Rossant, J., Hemberger, M., & Moffett, A. (2016). What is trophoblast? A combination of criteria define human first-trimester trophoblast. *Stem Cell Reports*, 6(2), 257–272.
29. Baergen, R. N., Burton, G. J., & Kaplan, C. G. (2021). *Benirschke's pathology of the human placenta* (7th ed). Springer Nature.
30. Okae, H., Toh, H., Sato, T., Hiura, H., Takahashi, S., Shirane, K., Kabayama, Y., Suyama, M., Sasaki, H., & Arima, T. (2018). Derivation of human trophoblast stem cells. *Cell Stem Cell*, 22(1), 50–63 e56.
31. Gestational hypertension and preeclampsia. (2020). Acog practice bulletin, number 222. *Obstetrics and Gynecology*, 135(6), e237–e260.
32. Dobbins, T. A., Sullivan, E. A., Roberts, C. L., & Simpson, J. M. (2012). Australian national birthweight percentiles by sex and gestational age, 1998–2007. *Medical Journal of Australia*, 197(5), 291–294.
33. Nguyen, A., Cannon, P., Kandel, M., Nguyen, T. V., Baird, L., Wong, G., Hannan, N. J., Tong, S., Bartho, L., & Kaitu'u-Lino, T. J. (2023). Cell surface associated protein mucin 15 (muc15) is elevated in preeclampsia. *Placenta*, 7(140), 39–46.
34. Fogarty, N. M., Ferguson-Smith, A. C., & Burton, G. J. (2013). Syncytial knots (tenney-parker changes) in the human placenta: Evidence of loss of transcriptional activity and oxidative damage. *American Journal of Pathology*, 183(1), 144–152.
35. Benirschke, K., Baergen, R. N., Burton, G., & Kaplan, C. G. (2021). *Benirschke's pathology of the human placenta* (7th ed.). Springer Nature.
36. Heumos, L., Schaar, A. C., Lance, C., Litnetskaya, A., Drost, F., Zappia, L., Lucken, M. D., Strobl, D. C., Henao, J., Curion, F., Single-cell Best Practices, C., Schiller, H. B., & Theis, F. J. (2023). Best practices for single-cell analysis across modalities. *Nat Reviews Genetics*, 24(8), 550–572.
37. Chang, C. W., & Parast, M. M. (2017). Human trophoblast stem cells: Real or not real? *Placenta*, 60(Suppl 1), S57–S60.
38. DiFederico, E., Genbacev, O., & Fisher, S. J. (1999). Preeclampsia is associated with widespread apoptosis of placental cytotrophoblasts within the uterine wall. *American Journal of Pathology*, 155(1), 293–301.
39. Huppertz, B. (2008). Placental origins of preeclampsia: Challenging the current hypothesis. *Hypertension*, 51(4), 970–975.
40. Langbein, M., Strick, R., Strissel, P. L., Vogt, N., Parsch, H., Beckmann, M. W., & Schild, R. L. (2008). Impaired cytotrophoblast cell-cell fusion is associated with reduced syncytin and increased apoptosis in patients with placental dysfunction. *Molecular Reproduction and Development*, 75(1), 175–183.
41. Sun, C., Groom, K. M., Oyston, C., Chamley, L. W., Clark, A. R., & James, J. L. (2020). The placenta in fetal growth restriction: What is going wrong? *Placenta*, 96, 10–18.
42. Wolmarans, E., Nel, S., Durandt, C., Mellet, J., & Pepper, M. S. (2018). Side population: Its use in the study of cellular heterogeneity and as a potential enrichment tool for rare cell populations. *Stem Cells International*, 2018, 2472137.
43. Sun, C., James, J. L., & Murthi, P. (2024). Three-dimensional in vitro human placental organoids from mononuclear villous trophoblasts or trophoblast stem cells to understand trophoblast dysfunction in fetal growth restriction. *Methods in Molecular Biology*, 2728, 235–245.
44. Richard, V., Nair, M. G., Santhosh Kumar, T. R., & Pillai, M. R. (2013). Side population cells as prototype of chemoresistant, tumor-initiating cells. *BioMed Research International*, 2013, 517237.

45. Liu, B. J., Xu, Q. Y., Yu, W. D., Li, N., Yao, T., Zhao, L. J., Wang, J. L., Wei, L. H., & Li, X. P. (2020). Study of the characterization of side population cells in endometrial cancer cell lines: Chemoresistance, progesterin resistance, and radioresistance. *Frontiers in Medicine (Lausanne)*, 7, 70.
46. Wang, M., Wang, Y., & Zhong, J. (2015). Side population cells and drug resistance in breast cancer. *Molecular Medicine Reports*, 11(6), 4297–4302.
47. Uezumi, A., Ojima, K., Fukada, S., Ikemoto, M., Masuda, S., Miyagoe-Suzuki, Y., & Takeda, S. (2006). Functional heterogeneity of side population cells in skeletal muscle. *Biochemical and Biophysical Research Communications*, 341(3), 864–873.
48. Singh, J. K., Simoes, B. M., Clarke, R. B., & Bundred, N. J. (2013). Targeting il-8 signalling to inhibit breast cancer stem cell activity. *Expert Opinion on Therapeutic Targets*, 17(11), 1235–1241.
49. Ortiz-Montero, P., Londono-Vallejo, A., & Vernot, J. P. (2017). Senescence-associated il-6 and il-8 cytokines induce a self- and cross-reinforced senescence/inflammatory milieu strengthening tumorigenic capabilities in the mcf-7 breast cancer cell line. *Cell Communication and Signaling: CCS*, 15(1), 17.
50. Redman, C. W., & Staff, A. C. (2015). Preeclampsia, biomarkers, syncytiotrophoblast stress, and placental capacity. *American Journal of Obstetrics and Gynecology*, 213(4 Suppl), S9 e1, S9-11.
51. Ferrari, F., Facchinetti, F., Saade, G., & Menon, R. (2016). Placental telomere shortening in stillbirth: A sign of premature senescence? *The Journal of Maternal-Fetal & Neonatal Medicine*, 29(8), 1283–1288.
52. Jovanovic, M., Stefanoska, I., Radojicic, L., & Vicovac, L. (2010). Interleukin-8 (cxcl8) stimulates trophoblast cell migration and invasion by increasing levels of matrix metalloproteinase (mmp)2 and mmp9 and integrins alpha5 and beta1. *Reproduction*, 139(4), 789–798.
53. Chen, Y., Zou, P., Bu, C., Jiang, Q., Xue, L., Bao, J., & Zhang, T. (2023). Upregulated cxcl8 in placenta accreta spectrums regulates the migration and invasion of htr-8/svneo cells. *Molecular Biology Reports*, 50(10), 8189–8199.
54. De Oliveira, L. G., Lash, G. E., Murray-Dunning, C., Bulmer, J. N., Innes, B. A., Searle, R. F., Sass, N., & Robson, S. C. (2010). Role of interleukin 8 in uterine natural killer cell regulation of extravillous trophoblast cell invasion. *Placenta*, 31(7), 595–601.
55. Sun, L., Mao, D., Cai, Y., Tan, W., Hao, Y., Li, L., & Liu, W. (2016). Association between higher expression of interleukin-8 (il-8) and haplotype -353a/-251a/+678t of il-8 gene with preeclampsia: A case-control study. *Medicine (Baltimore)*, 95(52), e5537.
56. Yue, S. L., Eke, A. C., Vaidya, D., Northington, F. J., Everett, A. D., & Graham, E. M. (2021). Perinatal blood biomarkers for the identification of brain injury in very low birth weight growth-restricted infants. *Journal of Perinatology*, 41(9), 2252–2260.
57. Martincic, K., Alkan, S. A., Cheate, A., Borghesi, L., & Milcarek, C. (2009). Transcription elongation factor ell2 directs immunoglobulin secretion in plasma cells by stimulating altered rna processing. *Nature Immunology*, 10(10), 1102–1109.
58. Founds, S. A., Conley, Y. P., Lyons-Weiler, J. F., Jeyabalan, A., Hogge, W. A., & Conrad, K. P. (2009). Altered global gene expression in first trimester placentas of women destined to develop preeclampsia. *Placenta*, 30(1), 15–24.
59. Shilatifard, A., Duan, D. R., Haque, D., Florence, C., Schubach, W. H., Conaway, J. W., & Conaway, R. C. (1997). Ell2, a new member of an ell family of rna polymerase ii elongation factors. *Proceedings of the National Academy of Sciences of the United States of America*, 94(8), 3639–3643.
60. Sakurai, K., Michiue, T., Kikuchi, A., & Asashima, M. (2004). Inhibition of the canonical wnt signaling pathway in cytoplasm: A novel property of the carboxyl terminal domains of two xenopus ell genes. *Zoological Science*, 21(4), 407–416.
61. Kaimakchiev, V., Terracciano, L., Tornillo, L., Spichtin, H., Stoios, D., Bundi, M., Korcheva, V., Mirlacher, M., Loda, M., Sauter, G., & Corless, C. L. (2004). The homeobox intestinal differentiation factor cdx2 is selectively expressed in gastrointestinal adenocarcinomas. *Modern Pathology*, 17(11), 1392–1399.
62. Suh, E., & Traber, P. G. (1996). An intestine-specific homeobox gene regulates proliferation and differentiation. *Molecular and Cellular Biology*, 16(2), 619–625.
63. Beck, F., Erler, T., Russell, A., & James, R. (1995). Expression of cdx-2 in the mouse embryo and placenta: Possible role in patterning of the extra-embryonic membranes. *Developmental Dynamics*, 204(3), 219–227.
64. DeWaal, D., Nogueira, V., Terry, A. R., Patra, K. C., Jeon, S. M., Guzman, G., Au, J., Long, C. P., Antoniewicz, M. R., & Hay, N. (2018). Hexokinase-2 depletion inhibits glycolysis and induces oxidative phosphorylation in hepatocellular carcinoma and sensitizes to metformin. *Nature Communications*, 9(1), 446.
65. Prater, M., Hamilton, R. S., Wa Yung, H., Sharkey, A. M., Robson, P., Abd Hamid, N. E., Jauniaux, E., Charnock-Jones, D. S., Burton, G. J., & Cindrova-Davies, T. (2021). Rna-seq reveals changes in human placental metabolism, transport and endocrinology across the first-second trimester transition. *Biology Open*, 10(6). <https://doi.org/10.1242/bio.058222>
66. He, J., Yang, H., Liu, Z., Chen, M., Ye, Y., Tao, Y., Li, S., Fang, J., Xu, J., Wu, X., & Qi, H. (2023). Elevated expression of glycolytic genes as a prominent feature of early-onset preeclampsia: Insights from integrative transcriptomic analysis. *Frontiers in Molecular Biosciences*, 10, 1248771.
67. Lv, H., Tong, J., Yang, J., Lv, S., Li, W. P., Zhang, C., & Chen, Z. J. (2018). Dysregulated pseudogene hk2p1 may contribute to preeclampsia as a competing endogenous rna for hexokinase 2 by impairing decidualization. *Hypertension*, 71(4), 648–658.
68. Wu, M., Liu, W., Huang, H., Chen, Z., Chen, Y., Zhong, Y., Jin, Z., Liu, X., & Zou, L. (2022). Pvt1/mir-145-5p/hk2 modulates vascular smooth muscle cells phenotype switch via glycolysis: The new perspective on the spiral artery remodeling. *Placenta*, 130, 25–33.
69. Wu, M., Liu, W., Huang, H., Chen, Z., Chen, Y., Zhong, Y., Jin, Z., Liu, X., & Zou, L. (2023). Corrigendum to pvt1/mir-145-5p/hk2 modulates vascular smooth muscle cells phenotype switch via glycolysis: The new perspective on the spiral artery remodeling [placenta 130 (2022) 25–33]. *Placenta*, 131, 71–74.
70. Guo, D., Meng, Y., Jiang, X., & Lu, Z. (2023). Hexokinases in cancer and other pathologies. *Cell Insight*, 2(1), 100077.
71. Lui, K. Y., Zhao, H., Qiu, C., Li, C., Zhang, Z., Peng, H., Fu, R., Chen, H. A., & Lu, M. Q. (2017). Integrator complex subunit 6 (ints6) inhibits hepatocellular carcinoma growth by wnt pathway and serve as a prognostic marker. *BMC Cancer*, 17(1), 644.
72. Ding, X., Chen, T., Shi, Q., Nan, P., Wang, X., Xie, D., & Li, J. (2021). Ints6 promotes colorectal cancer progression by activating of akt and erk signaling. *Experimental Cell Research*, 407(2), 112826.
73. Filleur, S., Hirsch, J., Wille, A., Schon, M., Sell, C., Shearer, M. H., Nelius, T., & Wieland, I. (2009). Ints6/dice1 inhibits growth of human androgen-independent prostate cancer cells by altering the cell cycle profile and wnt signaling. *Cancer Cell International*, 11(9), 28.
74. Arnholdt, H., Meisel, F., Fandrey, K., & Lohrs, U. (1991). Proliferation of villous trophoblast of the human placenta in normal and abnormal pregnancies. *Virchows Archiv B Cell Pathology Including Molecular Pathology*, 60(6), 365–372.

75. Ratajczak, M. Z., Ratajczak, J., & Kucia, M. (2019). Very small embryonic-like stem cells (vsels). *Circulation Research*, *124*(2), 208–210.
76. Bhartiya, D. (2017). Pluripotent stem cells in adult tissues: Struggling to be acknowledged over two decades. *Stem Cell Reviews and Reports*, *13*(6), 713–724.

**Publisher's Note** Springer Nature remains neutral with regard to jurisdictional claims in published maps and institutional affiliations.